analytical chemistry

Article

pubs.acs.org/ac

Highly Sensitive and Homogeneous Detection of Membrane Protein on a Single Living Cell by Aptamer and Nicking Enzyme Assisted Signal Amplification Based on Microfluidic Droplets

Lu Li, Qian Wang, Jie Feng, Lili Tong, and Bo Tang*

College of Chemistry, Chemical Engineering and Materials Science, Collaborative Innovation Center of Functionalized Probes for Chemical Imaging, Key Laboratory of Molecular and Nano Probes, Ministry of Education, Shandong Normal University, Jinan 250014, P. R. China

Supporting Information

ABSTRACT: Membrane proteins play vital roles in numerous physiological functions. Recently, they have been considered as candidate biomarkers for cancer and recognized as major drug targets. So, accurate, sensitive, and high-throughput quantitative detection of the membrane proteins is crucial for better understanding their roles in cancer cells and further validating their function in clinical research. Here, we report a highly sensitive and homogeneous detection of membrane protein on single living cells by aptamer and nicking enzyme assisted fluorescence signal amplification in microfluidic droplets. The homogeneous reaction based on the membrane protein-triggered conformation alteration of hairpin probe can improve the detection accuracy with elimination of several washing and separation steps. The microfluidic system provides a high-throughput platform for the detection of a single cell, and the highly monodisperse droplet can function as an independent microreactor for the aptamer and nicking enzyme assisted fluorescence signal amplification, coordinating with the small volume of the confined space (a droplet), increased reaction rate, and highly sensitive detection of membrane protein on single cell can be reached.

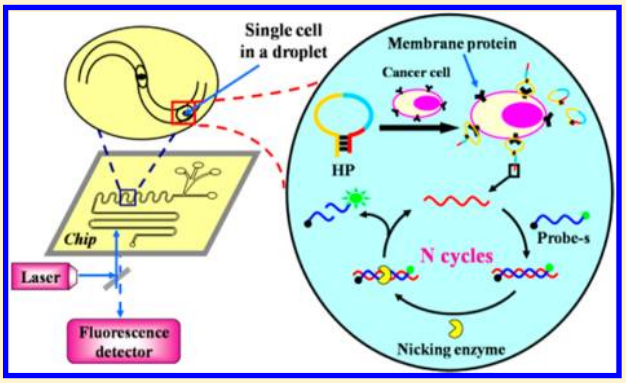

Membrane proteins, an essential part of biological membranes, comprise about half of the mass of biological membranes and play vital roles in numerous physiological functions, such as molecular recognition, energy transduction, and ion regulation.[1−4] A large number of human diseases have been linked to alterations in membrane proteins.[5,6] For example, the expression of membrane proteins may be altered during the transformation of a normal to a malignant cell.[3] Thus, membrane proteins have been considered as candidate biomarkers for cancer and recognized as major drug targets due to their accessibility. This subset of proteins actually represent more than 60% of the known existing and future drug targets.[4,7,8] Therefore, effective detection of membrane proteins is crucial for better understanding their roles in cancer cells and further validating their functions in clinical diagnosis. Currently, the enzyme-linked immunosorbent assay (ELISA), Western blot, and flow cytometry have been widely used for membrane proteins analysis.[9−12] ELISA is heterogeneous assay which requires complicated washing and separation process and may reduce the throughput as well as accuracy of the detection. The Western blot and flow cytometry can only achieve the half-quantitation of the protein and the sensitivity is still a restriction on the detection of the low-abundance membrane proteins. So, high-throughput, accurate, and sensitive quantitative detection of membrane proteins is in urgent need.

Recently, aptamers, a type of single-stranded RNA or DNA oligonucleotide analogues to antibodies, have been reported for the use of protein detection and other biological applications.[13−16] In comparison with the antibodies usually used for protein recognition, aptamers have significant advantages in which they offer higher binding specificity and affinity to the targets, potentially reduce immunogenicity, and increase tissue penetration associated with their small size.[17−19] They can also be chemically synthesized and easily modified.[20,21] These features make aptamers promising probes for molecular recognition, and the aptamer-based in situ detection of membrane proteins has been achieved. For example, Tan et al. successfully mapped membrane protein density on living cells using a FITC labeled aptamer.[22] Wang et al. reported an activatable aptamer probe for contrast-enhanced in vivo cancer imaging based on cell membrane protein-triggered conformation alteration.[23] Karp et al. developed cell-surface aptamer sensors to probe the cellular environments in real time.[24] In

Received: March 9, 2014
Accepted: April 29, 2014
Published: April 29, 2014

   dx.doi.org/10.1021/ac500881p | *Anal. Chem.* 2014, 86, 5101−5107

Scheme 1. (A) Schematic Representation of the Aptamer and Nicking Enzyme Assisted Signal Amplification Assay for Membrane Protein on Single Living Cells and (B) Basic Principle of Microfluidic Droplet System[a]

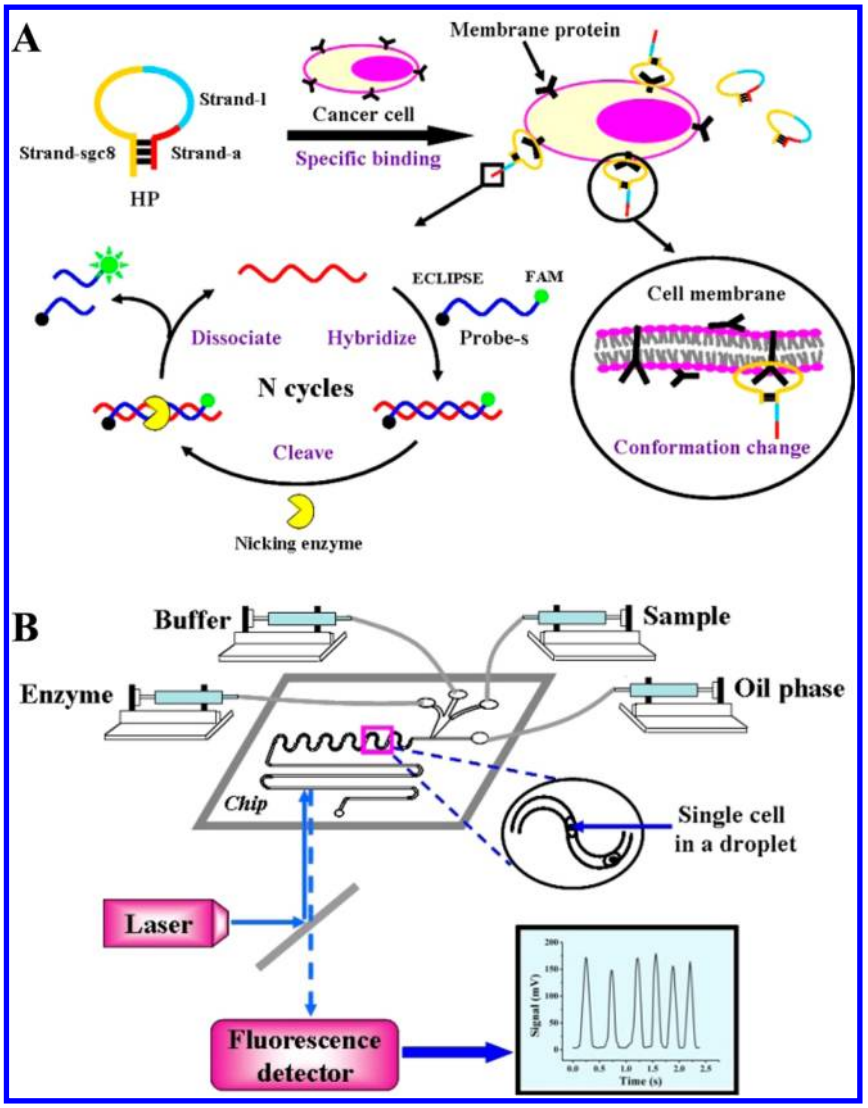

[a]The fluidic channel network consists of four inlets and one outlet. Three of the inlets are used to deliver aqueous solutions (enzyme, buffer and sample) and the fourth inlet delivers the water immiscible oil phase. The volumetric flows are controlled using the precision syringe pump containing four channels. A laser-induced fluorescence optical setup is used to focus the laser on the channel of the microfluidic system and collect the fluorescence arising from the cells in the droplets.

these methods, the signal of the target proteins was reported through the fluorescence of labeled organic dyes. Although developmental research is ongoing to enhance the fluorescence signal,[25−27] labeling with single or only a few dye molecules may limit the improvement in detection sensitivity. As a result, quantitative detection of membrane proteins can only be realized based on a large number of cells, and absolute quantity on a single living cell is still a great challenge.

Here, we report a highly sensitive and homogeneous detection of membrane protein on single living cells by an aptamer and nicking enzyme assisted fluorescence signal amplification in microfluidic droplets. The homogeneous reaction based on the membrane protein-triggered conformation alteration of a hairpin probe can improve the detection accuracy with elimination of several washing and separation steps. The microfluidic system provides a high-throughput platform for the detection of single cell, and the highly monodisperse droplet can function as an independent microreactor for the aptamer and nicking enzyme assisted fluorescence signal amplification, coordinating with the small volume of the confined space (a droplet), increased reaction rate, and highly sensitive detection of membrane protein on a single cell can be reached.

In the detection system, the cell membrane protein tyrosine kinase-7 (PTK7), an important biomarker receptor for T-cell acute lymphoblastic leukemia (T-ALL) cell line, was used as a model analyte.[28−30] In order to obtain high sensitivity, a strategy based on membrane protein-triggered conformation alteration of a hairpin probe and nicking enzyme assisted signal amplification was carried out. The detection principle is shown in Scheme 1A. The hairpin probe (HP) contains three fragments: an aptamer sgc8 that can interact with PTK7 specifically (strand-sgc8, yellow), a single-stranded poly-T DNA linker (strand-l, blue), and a DNA segment for amplification (strand-a, red). In the absence of protein, the hairpin probe was stable with the stem-loop structure as a result of the

dx.doi.org/10.1021/ac500881p | Anal. Chem. 2014, 86, 5101−5107

hybridization between part of the strand-sgc8 and its complementary part of the strand-a. After incubation with Hela cells, the aptamer could bind to the PTK7 on the cell membrane due to higher affinity, resulting in the conformation alteration of the HP and release of the strand-a. A short single-stranded signal probe (probe-s) consisting of the complementary sequence to strand-a and cleavage site for the nicking enzyme was employed for fluorescence detection through a fluorophore FAM and a quencher ECLIPSE attached at either terminal. First, the probe-s hybridized with the strand-a to form a double strand, which was a substrate of Nb.BbvCI. Then, the nicking enzyme bound to and only cleaved the probe-s. The cleaved probe-s was too short to maintain the double-stranded conformation. Consequently, the fluorophore was forced to separate far from the quencher, and a fluorescence signal was activated. The strand-a could be reused to hybridize to the next uncleaved probe-s. Finally, each strand-a could go through many cycles, and the fluorescence signal was amplified through continuous enzyme cleavage. Compared with traditional assays usually based on recognition interaction between target detection probe and membrane protein in a 1:1 stoichiometric ratio,[22−25,27] the proposed method has higher detection sensitivity due to the introduction of the circular signal amplification. Moreover, the aptamer-based approach can complete membrane protein analysis in a homogeneous format, resulting in the elimination of the washing and separation steps, which will be more convenient than the previously reported method.[31]

To achieve the high-throughput single-cell analysis, droplet-based microfluidic system was used to isolate single cell and provide small volume for the reaction compartments. The basic principle of microfluidic droplet system is shown in Scheme 1B. Hela cells incubated with HP and probe-s as sample were introduced into the microfluidic device together with the Nb.BbvCI solution (enzyme) and 1× NEbuffer 2 (buffer). Because of the pressure of the oil stream, monodisperse aqueous droplets formed and were snapped off at the microfluidic intersection. Accompanied by the moving of the droplets in the microchannel, the three suspensions were mixed inside the droplets, then nicking enzyme assisted signal amplification occurred in each droplet. Using a laser focused on the channel, the induced fluorescence from each droplet was quantified using a photomultiplier. This microfluidic system can support a high-throughput detection platform for single cell, and the highly monodisperse aqueous droplet can function as an independent microreactor. The picoliter volume of the droplet provided the advantage of about 100-fold increase in reaction speed accompanied by a remarkable reduction in reagent cost compared with a tube-based detection. The fluorescence products can be accumulated in the small confined space of droplets. A limit of detection as low as 0.4 nM was reached, and the absolute quantitation of PTK7 on single Hela cell surface has been achieved.

EXPERIMENTAL SECTION

Chemicals and Apparatus. Oligonucleotides HP (5′-ATCTAACTGCTGCGCCGCCGGGAAAATACTGTACGGTTAGATTTTTTTTTTTTTACCTCAGCAGTTAG-3′), probe-s (5′-6-FAM-TTCGCTGAGGAGC-ECLIPSE-3′) and HP-FAM (5′-ATCTAACTGCTGCGCCGCCGGGAAAATACTGTACGGTTAGATTTTTTTTTTTTTACCTCAGCAGTTAG-6-FAM-3′) were synthesized by Sangon Biotech Co., Ltd. (Shanghai, China). Nicking endonuclease Nb.BbvCI and buffer were purchased from New England Biolabs (Ipswich, MA). Bovine serum albumin was bought from Heowns Biochem Technologies (Tianjin, China). Human plasma fibronectin purified protein was purchased from Merck Millipore (Billerica, MA). Human PTK7 recombinant protein was produced by Abnova (Taipei, Taiwan). Tris, NaCl, and EDTA were purchased from Sigma-Aldrich (Shanghai, China). *N*-Tetradecane and span 80 were purchased from Aladdin (Shanghai, China). All chemicals and solvents used were of analytical grade. Deionized water was obtained through a Sartorius Arium 611 VF system (Sartorius AG, Germany) to a resistivity of 18.2 MΩ·cm.

Fluorescence measurements were carried out using a Cary Eclipse Fluorescence Spectrophotometer equipped with a xenon lamp and 1.0 cm quartz cells (Varian, CA). The signal produced by droplets was detected by the self-made laser-induced fluorescence detector (LIFD). The syringe pump containing four channels was made by Baoding Longer Precision Pump Co., Ltd. (Baoding, China).

Cell Culture and Treatment. Hela (cervix adenocarcinoma), CCRF-CEM (human leukemia), and Ramos (human Burkitt's lymphoma) cells were obtained from the Amercan Type Culture Collection (Manassas, VA). Cells were cultured in DMEM (Hyclone, U.S.A.) supplemented with 10% fetal bovine serum (Hyclone, U.S.A.), 100 U/mL penicillin, and 100 μg/mL streptomycin (Invitrogen, Carlsbad, CA) and incubated at 37 °C in a humidified atmosphere of 5% CO_2 and 95% air. The cells were collected and centrifuged at 1000 rpm for 5 min in culture medium, washed twice with PBS buffer, and then used for the membrane protein detection. The cell density was determined by a hemacytometer.

Reactions Based on Aptamer and Enzyme Amplification. Target protein PTK7 was dissolved in buffer and diluted to appropriate concentrations. The other reactants were diluted to corresponding concentration in 1× NEbuffer 2. The hairpin probe needed an annealing process before use. First of all, the hairpin probe was diluted to 1 μM using annealing buffer (10 mM Tris pH 8.0, 50 mM NaCl, 1 mM EDTA) and stayed at 95 °C for 2 min. Then the solution was slowly cooled to room temperature. The hairpin probe, probe-s, cell suspension, and PTK7 solution were mixed together and incubated at room temperature for 1 h. At last, Nb.BbvCI was added for the amplification reaction. The process was carried out at 37 °C for 30 min.

Fluorescence Measurements. After the reactions finished, the mixed solution was centrifuged at 1000 rpm for 5 min, and the supernatant was diluted to 200 μL with deionized water and moved to a quartz cell for fluorescence detection. The final solution contained 20 nM HP, 170 nM probe-s, 20 U/mL Nb.BbvCI and different concentrations of PTK7 in a volume of 200 μL. The samples were excited at 488 nm, and the emission spectra collection range was 500−580 nm. The fluorescence intensity at 518 nm was used to evaluate the performance of the proposed assay strategy. The excitation and emission slits used in the experiment were both 1.5 nm.

Microfluidic System. The microfluidic system consists of four main parts: a PDMS microchip, a syringe pump containing four channels, a laser-induced fluorescence detector (LIFD), and a data processing system. The PDMS microchip was designed by our research group and made by Wenhao Chip Technology Co., Ltd. (Suzhou, China). The depth of all the channels is 30 μm, and the diameter of all the ports is 1.5 mm. The microchip is 5 mm thick. The four inlets were, respectively,

dx.doi.org/10.1021/ac500881p | *Anal. Chem.* 2014, 86, 5101−5107

connected to 100 μL microsyringes on four channels of the syringe pump through PTFE pipes. The syringe pump was used to control the rates of liquid. The PDMS microchip was located on ax $X-Y-Z$ working platform of LIFD.

Generation of Droplets Containing Single Cells. *N*-Tetradecane with 2% span 80 surfactant was used as the oil phase. HP, probe-s, a certain number of cells, and different concentrations of PTK7 were mixed and incubated at room temperature for 1 h and the solution obtained from the reaction was worked as sample. The cell density was 2.5×10^6 cells/mL. The three aqueous channels were, respectively, imported the sample solution after reaction, buffer, and enzyme solution. The oil phase was injected at the rate of 2000 nL/min, and the three aqueous phases were all injected at the rate of 200 nL/min.

Laser-Induced Fluorescence Detection. A low-noise semiconductor double-pumped solid-state laser (MLLIII-473 nm/20 mW, Changchun Xinchanye Guangdianjishu Co. Ltd., China) was chosen. The laser position was adjusted on the channel. The fluorescence was finally detected by an R928 photomultiplier (PMT, Hamamatsu, Japan). Signal output of the PMT passing through the I/V converters (OPA128, BB Inc., U.S.A.) was collected using a CT-22 data acquisition card (the sampling frequency, 20 Hz, Shanghai Qianpu Shuju Co. Ltd., China). The computer incorporated with a program was used to control the PEPS and data acquisition.

RESULTS AND DISCUSSION

Verification of the Aptamer and Nicking Enzyme Assisted Signal Amplification. To illustrate the feasibility of the aptamer and nicking enzyme assisted signal amplification for membrane protein on cell surface, we first carried out the fluorescence detection of a large number of cells in solution. The signal amplification reaction was confirmed by the measurement of fluorescent spectra. The results are shown in Figure 1. The background fluorescence signal produced by 20 nM of the HP (group 2) was almost equivalent to the fluorescence intensity of cell suspension (group 1). After 170 nM of probe-s was added, the fluorescence intensity was still faint (group 3). Then, adding 20 U/mL of nicking enzyme, the fluorescence intensity displayed by group 4 was almost as low as the fluorescence without nicking enzyme (group 3). However, in the presence of 6.0×10^5 CCRF-CEM cells and Hela cells with PTK7 on their cell membranes, significant fluorescence response was achieved (groups 7 and 8). Although the protein density on CCRF-CEM cell surface is higher than that on Hela cell surface,[22] the Hela cell exhibits greater superficial area than the CCRF-CEM cell. The more PTK7 on Hela cells leads to stronger fluorescence. A control experiment on Ramos cells, which had been proved to be a negative control cell line for sgc8 binding,[32] was conducted and only faint fluorescence intensity was obtained (group 5). The low background fluorescence of the detection system and the remarkable fluorescence enhancement responding to the target protein indicate that the proposed strategy is successful and suitable for the analysis of membrane proteins. Another control experiment without signal amplification was also been conducted with the same amount of cells using the HP directly labeled with FAM (group 6). The stronger fluorescence obtained from the amplification reaction (group 8) illustrates the higher sensitivity of the proposed method.

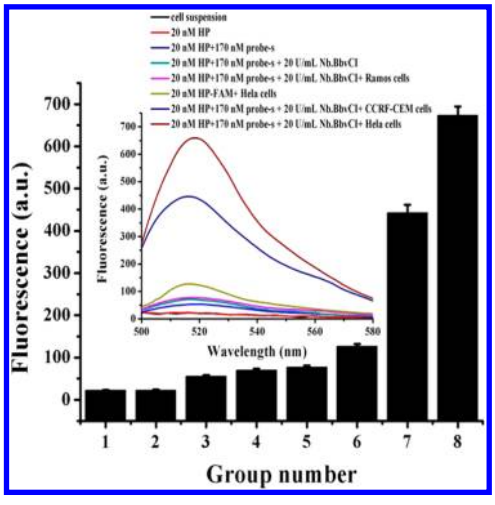

Figure 1. Fluorescence intensities of various phases in the assay. The components of the eight groups are 1, cell suspension; 2, HP; 3, HP and probe-s; 4, HP, probe-s, and Nb.BbvCI; 5, HP, probe-s, Nb.BbvCI, and Ramos cells; 6, HP-FAM and Hela cells; 7, HP, probe-s, Nb.BbvCI, and CCRF-CEM cells; 8, HP, probe-s, Nb.BbvCI, and Hela cells. The number of cells was 6.0×10^5. Error bars were estimated from three replicate measurements.

Evaluation of the Selectivity. The selectivity of the proposed method was investigated by adding the same amount of bovine serum albumin (BSA), human plasma fibronectin purified protein (Fn), and PTK7 into the cell suspension (each containing 1.7×10^5 cells), respectively. The results are shown in Figure 2, where F and F_0 are fluorescence intensities of amplification products in the presence and absence of Hela cells. Using a hairpin probe containing an aptamer sgc8 sequence with high affinity for PTK7, fluorescence intensity produced by PTK7 was approximately 26-fold of that produced by BSA and Fn. These results demonstrated that the fluorescence signal was specifically triggered by the aptamer/target binding for parallel samples. The excellent selectivity suggests that the proposed membrane protein detection method has potential applications in bioanalysis and clinical diagnosis.

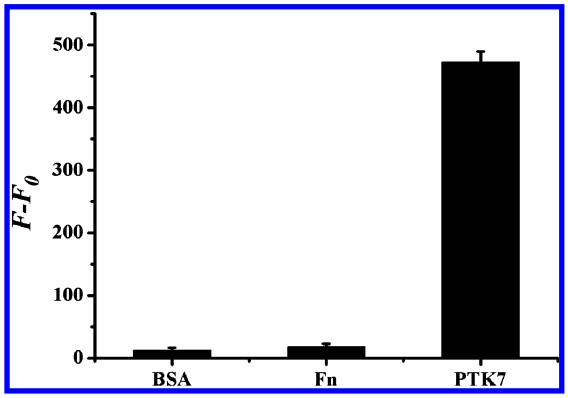

Figure 2. Comparison of the fluorescence intensity produced by BSA, Fn, and PTK7 using a hairpin probe containing an aptamer sgc8 sequence which has high affinity for PTK7, where F and F_0 are fluorescence intensities of amplification products in the presence and absence of Hela cells, respectively. The reaction solution contained 20 nM HP, 170 nM probe-s, 20 U/mL Nb.BbvCI, and 1.5 nM proteins. Error bars were estimated from three replicate measurements.

Quantitation of the Membrane Protein Based On a Large Number of Cells. In order to obtain optimal detection

dx.doi.org/10.1021/ac500881p | Anal. Chem. 2014, 86, 5101−5107

sensitivity, 20 nM HP, 170 nM probe-s, and 20 U/mL Nb.BbvCI were selected (Figure S1, Supporting Information). Under the optimized conditions, the sensitivity of the aptamer and enzyme assisted amplification assay for the PTK7 on the membrane of Hela cells was determined by the standard addition method using commercial PTK7 as standard. The fluorescence intensities via the reaction with different amounts of PTK7 added into the cell suspension were measured (Figure 3), and there was a remarkable increase with the higher amount

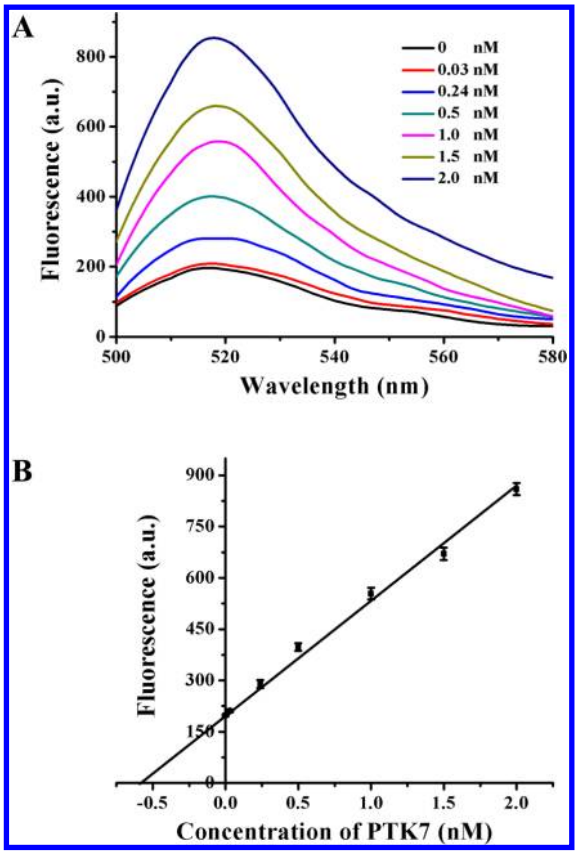

Figure 3. Standard addition method used for the determination of PTK7 in 1.7 × 10^5 cells. (A) Fluorescence emission spectra in the presence of increasing concentration of PTK7 (0, 0.03, 0.24, 0.5, 1.0, 1.5, and 2.0 nM). (B) The relationship between fluorescence intensity at λ_{em} = 518 nm and concentration of PTK7. Error bars were estimated from three replicate measurements.

of PTK7. A good linearity was obtained in 2 orders of magnitude from 30 pM to 2 nM PTK7. The correlation equation was $F = 199.33 + 335.27C$ (F represents fluorescence intensity of amplification products by the reaction in the presence of Hela cells; C represents the concentration of PTK7) with a correlation coefficient $R = 0.9941$. A relative standard deviation (RSD) of 2.1% for 11 repetitive measurements of 1.0 nM PTK7 was obtained, providing a good reproducibility of this assay. The detection limit was estimated to be 19 pM (LOD = 3σ/slope). According to the standard curve, the average amount of PTK7 on single cells was calculated to be 7.0 × 10^{-19} mol, which corresponds to the data obtained from the literature.[22]

Evaluation of the Droplet-Based Microfluidic System for Single-cell Detection. A droplet-based microfluidic system was established to perform the high-throughput single-cell analysis of the membrane protein. The production rate of the droplets and their volume are two key factors for the high throughput and sensitive detection. Especially, a well-defined droplet size can facilitate quantitative analysis of the target concentration in the droplet and thus allows more stringent and accurate detection. Through variation of the flow rates of the water phase and oil phase, it was possible to obtain continuous droplets with appropriate volume. The uniformity of droplet size and the reproducibility in their rate of formation could be assessed by performing a continued screening. From video 1 in the Supporting Information, we can see that droplets with a uniform length about 140 μm were steadily generated at a speed of 160 per minute. The volume of the droplets was calculated to be about 300 pL, which was suitable for the encapsulation of single cell. Laser-induced fluorescence detection was also carried out to profile the character of the droplets and further illustrate the applicability of the microfluidic system for fluorescence assay. After FITC was introduced into the water phase to form the fluorescent droplets, a laser-induced fluorescence optical setup was used to focus the laser on the channel of the microchip and gain the fluorescence signal. As shown in Figure 4, droplets can be

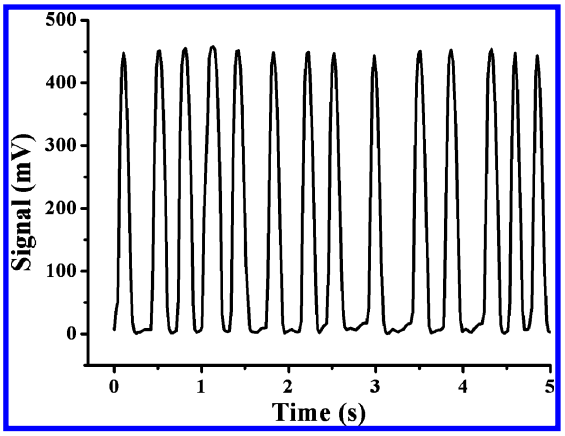

Figure 4. Optical readout of 5 s traces recorded. Each arch-shaped signal corresponds to the fluorescence of the aqueous droplet. The oil phase and aqueous phase speeds were 2000 nL/min and 200 nL/min, respectively.

distinguished by vertical spikes arising from the FITC. The uniform frequency of spikes indicated the steady droplet generation rate. The little variation in the height and area (RSD = 0.9% and 4.7%) of fluorescence bursts suggested the homogeneity in droplet size and space. The number of cells inside each droplet follows Poisson distribution. To ensure single-cell occupancy in the cell-containing droplets, we can estimate the number of cells per droplet using a Poisson distribution model, in which the probability $P(X = x)$ of finding x cells per droplet is given by the equation $P(X = x) = e^{-\lambda}[\lambda^x/x!]$, with λ representing the mean number of cells in the volume of each droplet.[33] As a result, cell encapsulation in the droplet can be tuned by changing the cell density in the aqueous phase. In the experiment, a density of 2.5 × 10^6 cells/mL was used. Considering that the cell encapsulation process is completely random, this choice of cell density will result in 77.88% of the droplets containing no cells, 19.47% containing a single cell, 2.43% containing two cells, and 0.22% containing more than two cells. Under this concentration, we successfully fabricated droplets at a mean rate of 41 droplets containing single cell per minute and a typical movie that shows the process of cell

dx.doi.org/10.1021/ac500881p | Anal. Chem. 2014, 86, 5101−5107

encapsulation is exhibited in the Supporting Information (video 2). All the above results illustrate that the established droplet-based microfluidic system allows high-throughput analysis of the membrane protein at the single-cell level in a highly uniform and reproducible manner.

Reaction Kinetics of the Enzyme-Based Signal Amplification of a Single Cell in a Droplet. To form droplets from the sample and enzyme solutions without bringing the reagents into prior contact, the two solutions were flowed in microchannels as two laminar streams and another buffer was delivered into the middle aqueous inlet as an inert center stream to separate them. Diffusion through the central stream was too slow for the reagents in the two side streams to interact prior to the formation of a droplet.[34] Thus, mixing of the three solutions only occurred inside the droplet. By inducing a winding part into the microchannel, mixing inside droplets is enhanced by chaotic advection, which can be as fast as a few milliseconds.[35] In the microfluidic system, each aqueous droplet functions as an independent microreactor. Because the volume of each droplet is restricted and no reagents disperse, signal molecules generated by an individual cell can rapidly attain high concentrations of solutes. The reaction kinetics of the enzyme-based signal amplification of a single cell in a droplet has also been demonstrated for performing rapid fluorescence measurements at different points of the microchannel. The spatial dimension can be converted to reaction time by accounting for the linear flow velocity within the fluidic channel. As shown in Figure 5, the fluorescence

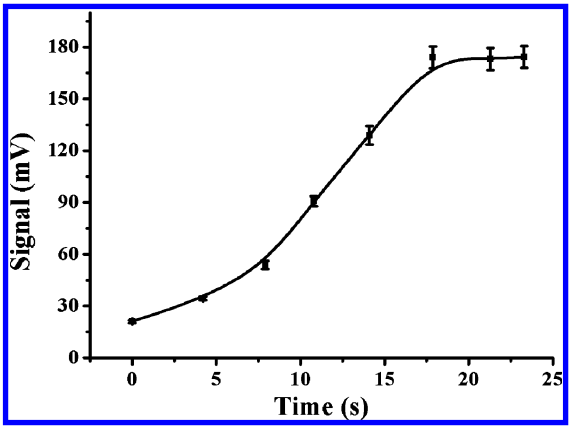

Figure 5. Kinetics curve illustrating the fluorescence intensity as a function of the enzyme reaction time in the presence of single cells. The fluorescence intensity was obtained at different points of the microchannel. The final concentrations of HP and probe-s were, respectively, 20 nM and 170 nM. Error bars were estimated from three replicate measurements.

intensity is nearly constant after 17 s, implying the amplification reaction in the droplets could finish within a very short time. Compared to 30 min in the tube (Figure S2, Supporting Information), there was an increase of 2 orders of magnitude in the reaction rate in droplets. Because of the rapid mixing and the enrichment of the fluorescent products in small volume, a high sensitivity of the membrane protein detection can be reached effectively using this droplet-based microfluidic system.

Quantitation of the Membrane Protein on Single Cells. To characterize the proposed method, we analyzed the expression of membrane protein PTK7 on Hela cells. After cells and reagents were isolated in the droplet, fluorescence detection could be accomplished quickly using the laser focusing on the end of channel without extra incubation. The signal acquired for 10 s is shown in Figure 6. The separated

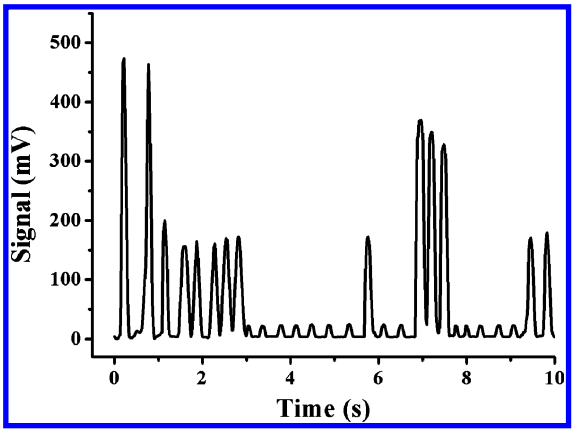

Figure 6. Optical readout of 10 s traces recorded. Each arch-shaped signal corresponds to the fluorescence of the aqueous droplet.

vertical spike represented the signal arising from single droplet. The discontinuous variety in the intensity from 0 to 500 mV can be explained by the random cell encapsulation process. Although there is discrepancy in the encapsulation probability of single cell in droplets between the calculation and the observation from the 28 droplets in Figure 6, the statistical data obtained from thousands of droplets are almost similar to the calculation results based on a Poisson distribution model. When there were no cells in the droplet, only faint signal from the background was detected. The frequent intensity around 150 mV corresponded to the products arising from single cell encapsulated in a droplet and the stronger intensity above 300 arose from more than one cell in a droplet. The amount of PTK7 on the single Hela cell was determined using the standard curve (Figure S3 in the Supporting Information). It was calculated to be 5.7×10^{-19} to $\sim 7.9 \times 10^{-19}$ mol/cell that is corresponding to the data obtained from the tube-based detection above. The fluorescence signal corresponding to the expression of PTK7 on a single CCRF-CEM cell is also shown in Figure S4 in the Supporting Information.

CONCLUSIONS

In conclusion, we constructed a highly sensitive detection system for membrane protein on individual cell using aptamer and enzyme assisted amplification inside microfluidic droplets. The aptamer-based strategy can complete protein analysis in a homogeneous format, eliminating the washing and separation steps, and the enzyme assisted circular signal amplification can lead to high sensitivity. Using the droplet-based microfluidic technology, rapid reaction rate and amazing detection sensitivity have been reached further due to the isolated, small volume of the droplets. Finally, high throughput single-cell analysis of the low-abundance biomarker PTK7 was carried out. The method is universal for other membrane proteins on the cell surface and possesses potential application in medical research and early clinical diagnostics.

ASSOCIATED CONTENT

Supporting Information

Supplementary figures S1−S3 and videos 1 and 2. This material is available free of charge via the Internet at http://pubs.acs.org.

dx.doi.org/10.1021/ac500881p | Anal. Chem. 2014, 86, 5101−5107

AUTHOR INFORMATION

Corresponding Author

*E-mail: tangb@sdnu.edu.cn.

Notes

The authors declare no competing financial interest.

ACKNOWLEDGMENTS

This work was supported by the 973 Program (Grant 2013CB933800), National Natural Science Foundation of China (Grants 21227005, 21390411, 91313302, 21035003, and 21205074), Program for Changjiang Scholars and Innovative Research Team in University and the Shandong Distinguished Middle-Aged and Young Scientist Encourage and Reward Foundation (Grant BS2012SW022).

REFERENCES

(1) Marmagne, A.; Rouet, M. A.; Ferro, M.; Rolland, N.; Alcon, C.; Joyard, J.; Garin, J.; Barbier-Brygoo, H.; Ephritikhine, G. *Mol. Cell. Proteomics* **2004**, *3*, 675−691.

(2) Schindler, J.; Lewandrowski, U.; Sickmann, A.; Friauf, E.; Nothwang, H. G. *Mol. Cell. Proteomics* **2006**, *5*, 390−400.

(3) Grimm, D.; Bauer, J.; Pietsch, J.; Infanger, M.; Eucker, J.; Eilles, C.; Schoenberger, J. *Curr. Med. Chem.* **2011**, *18*, 176−190.

(4) Arinaminpathy, Y.; Khurana, E.; Engelman, D. M.; Gerstein, M. B. *Drug Discovery Today* **2009**, *14*, 1130−1135.

(5) Brown, D. M.; Ruoslahti, E. *Cancer Cell* **2004**, *5*, 365−374.

(6) Sanders, C. R.; Nagy, J. K. *Curr. Opin. Struct. Biol.* **2000**, *10*, 438−442.

(7) Ghirlanda, G. *Curr. Opin. Chem. Biol.* **2009**, *13*, 643−651.

(8) Yildirim, M. A.; Goh, K. I.; Cusick, M. E.; Barabasi, A. L.; Vidal, M. *Nat. Biotechnol.* **2007**, *25*, 1119−1126.

(9) Baskar, S.; Kwong, K. Y.; Hofer, T.; Levy, J. M.; Kennedy, M. G.; Lee, E.; Staudt, L. M.; Wilson, W. H.; Wiestner, A.; Rader, C. *Clin. Cancer Res.* **2008**, *14*, 396−404.

(10) Cheng, A.; McDonald, N. A.; Connolly, C. N. J. *Biol. Chem.* **2005**, *280*, 22502−22507.

(11) Kaur, J.; Bachhawat, A. K. *Anal. Biochem.* **2009**, *384*, 348−349.

(12) Ducrest, A. L.; Amacker, M.; Lingner, J.; Nabholz, M. *Nucleic Acids Res.* **2002**, *30*, e65.

(13) Stojanovic, M. N.; Landry, D. W. *J. Am. Chem. Soc.* **2002**, *124*, 9678−9679.

(14) Minunni, M.; Tombelli, S.; Gullotto, A.; Luzi, E.; Mascini, M. *Biosens. Bioelectron.* **2004**, *20*, 1149−1156.

(15) de-los-Santos-Alvarez, N.; Lobo-Castanon, M. J.; Miranda-Ordieres, A. J.; Tunon-Blanco, P. *J. Am. Chem. Soc.* **2007**, *129*, 3808−3809.

(16) Rupcich, N.; Nutiu, R.; Li, Y.; Brennan, J. D. *Angew. Chem., Int. Ed.* **2006**, *45*, 3295−3299.

(17) Liu, J.; Cao, Z.; Lu, Y. *Chem. Rev.* **2009**, *109*, 1948−1998.

(18) Fang, X.; Tan, W. *Acc. Chem. Res.* **2010**, *43*, 48−57.

(19) Famulok, M.; Hartig, J. S.; Mayer, G. *Chem. Rev.* **2007**, *107*, 3715−3743.

(20) Keefe, A. D.; Pai, S.; Ellington, A. *Nat. Rev. Drug Discovery* **2010**, *9*, 537−550.

(21) Cho, E. J.; Lee, J. W.; Ellington, A. D. *Annu. Rev. Anal. Chem.* **2009**, *2*, 241−264.

(22) Chen, Y.; Munteanu, A. C.; Huang, Y. F.; Phillips, J.; Zhu, Z.; Mavros, M.; Tan, W. *Chemistry* **2009**, *15*, 5327−5336.

(23) Shi, H.; He, X.; Wang, K.; Wu, X.; Ye, X.; Guo, Q.; Tan, W.; Qing, Z.; Yang, X.; Zhou, B. *Proc. Natl. Acad. Sci. U.S.A.* **2011**, *108*, 3900−3905.

(24) Zhao, W.; Schafer, S.; Choi, J.; Yamanaka, Y. J.; Lombardi, M. L.; Bose, S.; Carlson, A. L.; Phillips, J. A.; Teo, W.; Droujinine, I. A.; Cui, C. H.; Jain, R. K.; Lammerding, J.; Love, J. C.; Lin, C. P.; Sarkar, D.; Karnik, R.; Karp, J. M. *Nat. Nanotechnol.* **2011**, *6*, 524−531.

(25) Yin, J.; He, X.; Wang, K.; Qing, Z.; Wu, X.; Shi, H.; Yang, X. *Nanoscale* **2012**, *4*, 110−112.

(26) Zhu, G.; Zhang, S.; Song, E.; Zheng, J.; Hu, R.; Fang, X.; Tan, W. *Angew. Chem., Int. Ed.* **2013**, *52*, 5490−5496.

(27) Yin, J.; He, X.; Wang, K.; Xu, F.; Shangguan, J.; He, D.; Shi, H. *Anal. Chem.* **2013**, *85*, 12011−12019.

(28) Mossie, K.; Jallal, B.; Alves, F.; Sures, I.; Plowman, G. D.; Ullrich, A. *Oncogene* **1995**, *11*, 2179−2184.

(29) Easty, D. J.; Mitchell, P. J.; Patel, K.; Florenes, V. A.; Spritz, R. A.; Bennett, D. C. *Int. J. Cancer* **1997**, *71*, 1061−1065.

(30) Shangguan, D.; Cao, Z.; Meng, L.; Mallikaratchy, P.; Sefah, K.; Wang, H.; Li, Y.; Tan, W. *J. Proteome Res.* **2008**, *7*, 2133−2139.

(31) Joensson, H. N.; Samuels, M. L.; Brouzes, E. R.; Medkova, M.; Uhlen, M.; Link, D. R.; Andersson-Svahn, H. *Angew. Chem., Int. Ed.* **2009**, *48*, 2518−2521.

(32) Shangguan, D.; Li, Y.; Tang, Z.; Cao, Z. C.; Chen, H. W.; Mallikaratchy, P.; Sefah, K.; Yang, C. J.; Tan, W. *Proc. Natl. Acad. Sci. U.S.A.* **2006**, *103*, 11838−11843.

(33) Mazutis, L.; Gilbert, J.; Ung, W. L.; Weitz, D. A.; Griffiths, A. D.; Heyman, J. A. *Nat. Protoc.* **2013**, *8*, 870−891.

(34) Song, H.; Tice, J. D.; Ismagilov, R. F. *Angew. Chem., Int. Ed.* **2003**, *42*, 768−772.

(35) Srisa-Art, M.; Dyson, E. C.; deMello, A. J.; Edel, J. B. *Anal. Chem.* **2008**, *80*, 7063−7067.